Journal of Sound and Vibration 329 (2010) 328–337

Contents lists available at ScienceDirect

Journal of Sound and Vibration

journal homepage: www.elsevier.com/locate/jsvi

Thermoelastic damping in micro-scale circular plate resonators

Yuxin Sun [a,b,*], Masumi Saka [b]

[a] The Solid Mechanics Research Centre, Beijing University of Aeronautics and Astronautics, Beijing 100191, PR China
[b] Department of Nanomechanics, Tohoku University, Aoba 6-6-01, Aramaki, Aoba-ku, Sendai 980-8579, Japan

ARTICLE INFO

Article history:
Received 22 July 2008
Received in revised form
9 September 2009
Accepted 11 September 2009
Handling Editor: L.G. Tham

ABSTRACT

The governing equations of coupled thermoelastic problems are established for out-of-plane vibration of a circular plate. The analytical expression for thermoelastic damping is obtained. Then the thermoelastic damping is studied under different environmental temperature, plate dimensions and boundary conditions.

1. Introduction

Micro-scale mechanical resonators have high sensitivity as well as fast response [1,2] and are widely used as sensors and modulators [3,4]. It is necessary to know how the parameters affect their physical and mechanical behaviors. For resonators, it is desired to design and construct systems with loss of mechanical energy as little as possible. Unfortunately, it has been consistently observed that there exists energy dissipation that increases with size decreasing significantly – even when made from pure single-crystal materials [5]. Many researchers have discussed different dissipation mechanisms in MEMS [6–9], such as doping-impurities losses, support-related losses and thermoelastic damping, as well as the radiation of energy away from the resonator into its surroundings.

Thermoelastic damping is an inherent energy dissipation mechanism in micromechanical resonators. Thermoelastic damping arises from thermal currents generated by contraction/extension in elastic media. The bending of the reed causes dilations of opposite signs to exist on the upper and lower halves. One side is compressed and heated, and the other side is stretched and cooled. Thus, in the presence of finite thermal expansion, a transverse temperature gradient is produced. The temperature gradient generates local heat currents, which cause increase of the entropy of the reed and lead to energy dissipation. The temperature across the reed equalizes in a characteristic time τ_R, while the vibration frequency of the reed is ω. In the low-frequency range, i.e., $\tau_R \ll \omega^{-1}$, the vibrations are isothermal and a small amount of energy is dissipated. On the other hand, for $\tau_R \gg \omega^{-1}$, adiabatic conditions prevail with low-energy dissipation similar to the low-frequency range. While $\tau_R \approx \omega^{-1}$, stress and strain are out of phase and a maximum of internal friction occurs. This is the so-called Debye peak.

Zener [10,11] firstly predicted the existence of the thermoelastic damping process. Further experiments consistent with Zener's theory were provided by Berry [12] for α-brass, in which case the damping was measured as a function of frequency at room temperature. Roszhardt [13] and Yasumura et al. [14] observed thermoelastic damping in single-crystal silicon and silicon nitride micro-resonators at room temperature, respectively. Houston et al. [15] found that the internal friction arising from thermoelastic damping is strong and persists down to 50 nm scale structures in silicon-based MEMS. Lifshitz

* Corresponding author at: The Solid Mechanics Research Centre, Beijing University of Aeronautics and Astronautics, Beijing 100191, PR China.
E-mail address: yxsun@buaa.edu.cn (Y. Sun).

0022-460X/$ - see front matter © 2009 Elsevier Ltd. All rights reserved.
doi:10.1016/j.jsv.2009.09.014

and Roukes [5] studied thermoelastic damping of a beam with rectangular cross-sections, and found that after the Debye peaks, the thermoelastic attenuation will be weakened as the size increases. In addition, Srikar and Senturia [16] studied thermoelastic damping in fine-grained polysilicon flexural beam resonators. Wong et al. [17] considered thermoelastic damping of the in-plane vibration of thin silicon rings of rectangular cross-section. De and Aluru [18] modified the classical theory of thermoelastic damping for application to electrostatically actuated microstructures by taking into account the nonlinear nature of the electrostatic force. Nayfeh and Younis [19] presented a model and analytical expressions for the quality factors of microplate of general shapes due to thermoelastic damping. The above papers used the quasi-1-D theory as their basis. Recently, Prabhakar and Vengallatore [20] developed a 2-D theory for thermoelastic damping in Euler–Bernoulli beams. Since the models of Zener and Lifshitz and Roukes are now widely used to estimate thermoelastic damping in micro-resonators, this paper will still start from the quasi-1-D theory.

This paper deals with thermoelastic damping effects on the out-of-plane vibration of circular plate resonators. Circular plates are common elements in many sensors and resonators [21]. For example, Vig et al. [22] proposed a micro-resonator based high sensitivity sensor and sensor array for use as infrared (IR) sensors. Microscale-circular resonators may have thickness of 1–10 μm and diameter of 100–1000 μm, with resonance frequencies of the fundamental mode (thickness shear mode) in the range of 100–1000 MHz. Although such micro-resonators are not suitable for precision frequency control applications due to their extremely high sensitivity to mass loading, they can be used for IR detection and imaging, and for chemical and biological agent sensing. In particular, when quartz is used as the resonator material, the temperature dependence of the resonance frequency can be utilized to make precision thermometers [23,24].

Such resonators can be considered as a thin circular plate. So the governing equation of the thermoelastic coupling problem for this resonator can be derived through thin plate theory in cylindrical coordinates. In the previous work [25], we studied thermoelastic damping of the axisymmetric vibration in circular plates. This paper will study thermoelastic damping of the vibration in arbitrary direction in circular plates.

2. Problem formulation

Consider a thin circular plate with uniform thickness h and radius a. The cylindrical coordinate system (r,θ,z) is applied to study the vibration of the circular plate, with an origin located at the center of the plate. We put the neutral surface on the (r,θ) coordinate plane, and the z-axis normal to the neutral surface. We define $w(r,\theta,t)$ and $T(r,\theta,z,t)$ to be the axial or out-of-plane displacement and the temperature field, respectively. In equilibrium, the plate is unstrained, unstressed, and keeps at the environmental temperature T_0 everywhere. Assuming small strains and displacements, and considering the Kirchhoff–Love plate theory, we can obtain the differential equation of the vibration of the microplate as [25]

$$D\nabla^2\nabla^2 w + D(1+\nu)\alpha_T\nabla^2 M_T + \rho h\frac{\partial^2 w}{\partial t^2} = 0, \tag{1}$$

where t is the time, ρ, ν and α_T are the density, the Poisson ratio and the coefficient of thermal expansion, respectively, $D=Eh^3/[12(1-\nu^2)]$ is the plate flexural rigidity, in which E is the Young's modulus; $M_T=(12/h^3)\int_{-h/2}^{h/2}\vartheta z\,dz$ is the thermal moment, in which $\vartheta=T-T_0$ is the temperature increment; ∇^2 is the Laplace operator in the polar coordinate system, as is expressed in the following:

$$\nabla^2 = \frac{\partial^2}{\partial r^2} + \frac{1}{r}\frac{\partial}{\partial r} + \frac{1}{r^2}\frac{\partial^2}{\partial\theta^2}. \tag{2}$$

The thermal conduction equation containing the thermoelastic coupling term has the following form [25]:

$$\kappa\nabla^2\vartheta + \kappa\frac{\partial^2\vartheta}{\partial z^2} = \rho c_v\frac{\partial\vartheta}{\partial t} - \beta T_0 z\frac{\partial}{\partial t}(\nabla^2 w), \tag{3}$$

where c_v is the specific heat at constant volume, κ the thermal conductivity and $\beta=E\alpha_T/(1-2\nu)$ the thermal modulus.

We plan to formulate and solve the thermoelastic coupling problem using the standard approach as was used by Lifshitz and Roukes for deriving thermoelastic damping in a beam resonator [5]. So we make some simplification in the thermal conduction equation. Noting that thermal gradients in the plane of the cross-section along the plate thickness direction are much larger than gradients along the radial direction, we can ignore the term $\nabla^2\vartheta$ in the thermal conduction equation. That is to say, the thermal conduction equation can be simplified as

$$\kappa\frac{\partial^2\vartheta}{\partial z^2} = \rho c_v\frac{\partial\vartheta}{\partial t} - \beta T_0 z\frac{\partial}{\partial t}(\nabla^2 w). \tag{4}$$

In summary, we can get the governing equations of this problem composed of Eqs. (1) and (4).

In general, the elastic and thermal properties of silicon are temperature dependent. However, the temperature change associated with thermoelastic vibration is known to be small ($\ll 1$ K) [17] and it is therefore reasonable to treat the mechanical and thermal parameters as constants with values applicable to the environmental temperature T_0.

3. Solution of the governing equations

To calculate the effect of thermoelastic coupling on the vibrations of a circular plate, we solve the coupled thermoelastic Eqs. (1) and (4) for the case of harmonic vibrations. We set

$$w(r,\theta,t)=\sum_{m=1}^{\infty}\sum_{n=0}^{\infty}W_{nm}(r)e^{i(\omega_{nm}t+n\theta)},\ \vartheta(r,\theta,z,t)=\sum_{m=1}^{\infty}\sum_{n=0}^{\infty}\Theta_{nm}(r,z)e^{i(\omega_{nm}t+n\theta)}, \tag{5}$$

where ω_{nm} is the frequency and $W_{nm}(r)e^{in\theta}$ the mode shape of the displacement. In the notation used here, n=0,1,2,… denoted the number of nodal diameters and m=1,2,… the number of nodal circles [26]. We expect to find that in general the frequency ω_{nm} is complex, the real part $\mathrm{Re}(\omega_{nm})$ giving the new eigen-frequencies of the plate in the presence of thermoelastic coupling effect, and the imaginary part $|\mathrm{Im}(\omega_{nm})|$ giving the attenuation of the vibration.

Substituting Eq. (5) into Eqs. (1) and (4) yields the following equations:

$$D\nabla^{*2}\nabla^{*2}W_{nm}+D(1+\nu)\alpha_T\nabla^{*2}M_{T0}-\rho h\omega_{nm}^2W_{nm}=0, \tag{6}$$

$$\kappa\frac{\partial^2\Theta_{nm}}{\partial z^2}=i\omega_{nm}\rho c_\nu\Theta_{nm}-i\omega_{nm}\beta T_0 z\nabla^{*2}W_{nm}, \tag{7}$$

where

$$\nabla^{*2}=\frac{\partial^2}{\partial r^2}+\frac{1}{r}\frac{\partial}{\partial r}-\frac{n^2}{r^2}, \tag{8}$$

$$M_{T0}=\frac{12}{h^3}\int_{-h/2}^{h/2}\Theta_{nm}(r,z)z\,\mathrm{d}z. \tag{9}$$

There is no flow of heat across the upper and lower surfaces of the plate, that is, $\partial\Theta_{nm}/\partial z$=0 at $z=\pm h/2$. Then, the solution of Eq. (7) can be obtained as

$$\Theta_{nm}(r,z)=\frac{\beta T_0}{\rho c_\nu}\nabla^{*2}W_{nm}\left(z-\frac{\sin(Nz)}{N\cos(Nh/2)}\right), \tag{10}$$

where

$$N=(1-i)\sqrt{\frac{\omega\rho c_\nu}{2\kappa}}, \tag{11}$$

where i is the square root of -1.

Substitution of Eqs. (9) and (10) into Eq. (6) gives

$$D_\omega\nabla^2\nabla^2W_{nm}-\rho h\omega_{nm}^2W_{nm}=0, \tag{12}$$

where

$$D_\omega=D(1+\Delta_D(1+f(\omega_{nm}))), \tag{13}$$

$$\Delta_D=\frac{(1+\nu)\alpha_T\beta T_0}{\rho c_\nu}, \tag{14}$$

$$f(\omega_{nm})=\frac{24}{N^3h^3}\left(\frac{Nh}{2}-\tan\left(\frac{Nh}{2}\right)\right). \tag{15}$$

Considering the limitation of $W_{nm}(r)$ at the plate center (r=0), we can get the solution of Eq. (12) as

$$W_{nm}(r)=C_1J_n(pr)+C_2I_n(pr), \tag{16}$$

where $p^4=\rho h{\omega_{nm}}^2/D_\omega$, and the coefficients C_1 and C_2 are governed by the boundary conditions.

In this paper, two kinds of boundary conditions are considered. On the one hand, boundary conditions regarding movements in the case of a clamped plate have the form of

$$\begin{cases}W_{nm}|_{r=a}=0,\\ \dfrac{dW_{nm}}{dr}|_{r=a}=0.\end{cases} \tag{17}$$

Substitute expression of deflection, i.e., Eq. (16), into the boundary conditions, i.e., Eq. (17), we have

$$\begin{cases}C_1J_n(pa)+C_2I_n(pa)=0,\\ C_1p[-J_{n+1}(pa)+(n/pa)J_n(pa)]+C_2p[I_{n+1}(pa)+(n/pa)I_n(pa)]=0.\end{cases} \tag{18}$$

Table 1
Values of q_{nm} (n=0, 1, 2, 3 and m=1, 2, 3) for the clamped and simply supported plates.

n	Clamped			Simply supported		
	q_{n1}	q_{n2}	q_{n3}	q_{n1}	q_{n2}	q_{n3}
0	10.2158	39.7711	89.1041	5.7832	30.4713	74.8870
1	21.2604	60.8287	120.0792	14.6820	49.2185	103.4995
2	34.8770	84.5826	153.8151	26.3746	80.8500	135.0207
3	51.0300	111.0214	190.3038	40.7065	95.2776	169.3954

In order to get nontrivial solutions, the constants C_1 and C_2 must be nonzero. Therefore, we obtain the following frequency equation:

$$\begin{vmatrix} J_n(pa) & I_n(pa) \\ -J_{n+1}(pa)+(n/pa)J_n(pa) & I_{n+1}(pa)+(n/pa)I_n(pa) \end{vmatrix} = 0. \tag{19}$$

The allowed value of pa may be obtained through solving Eq. (19) as $pa=\sqrt{q_{nm}}$, where the values of q_{nm} (n=0, 1, 2, 3, m=1, 2, 3) are listed in Table 1.

On the other hand, in the case of a simply supported plate, the boundary conditions become

$$\begin{cases} W_{nm}|_{r=a}=0, \\ [\nabla^{*2}W_{nm}+(1+\nu)\alpha_T M_{T0}]|_{r=a}=0. \end{cases} \tag{20}$$

According to Eqs. (9) and (10), the above boundary conditions can be changed to

$$\begin{cases} W_{nm}|_{r=a}=0, \\ \nabla^{*2}W_{nm}|_{r=a}=0. \end{cases} \tag{21}$$

Substituting Eq. (16) into Eq. (21) yields the following frequency equation:

$$\begin{vmatrix} J_n(pa) & I_n(pa) \\ -J_n(pa) & I_n(pa) \end{vmatrix} = 0, \tag{22}$$

The solution of Eq. (22) is $pa=\sqrt{q_{nm}}$, with the values of q_{nm} (n=0, 1, 2, 3, m=1, 2, 3) listed in Table 1.

From Eqs. (16), (19) and (22), we can obtain the mode shape of the clamped and the simply supported plate, respectively. To provide some intuition, we plot the first few (n, m) mode shapes of a simply supported circular plate in Fig. 1.

Now the vibration frequency of the circular plate considering thermoelastic coupling effect can be obtained as

$$\omega_{nm}=p^2\sqrt{\frac{D_\omega}{\rho h}}=\omega_0\sqrt{1+\Delta_D(1+f(\omega_{nm}))}, \tag{23}$$

where ω_0 is the eigenfrequency when thermoelastic coupling effect is ignored with the expression of

$$\omega_0=\frac{q_{nm}}{a^2}\sqrt{\frac{D}{\rho h}}. \tag{24}$$

Noting that $\Delta_D \ll 1$ for silicon (Δ_D=1.26 × 10^{-4} for T_0=293 K), we can replace $f(\omega)$ in the square root by $f(\omega_0)$ and expand Eq. (23) into a series up to first order. Then Eq. (23) becomes

$$\omega_{nm}=\omega_0\left[1+\frac{\Delta_D}{2}(1+f(\omega_0))\right]. \tag{25}$$

By the convenient substitution

$$\xi=h\sqrt{\frac{\omega_0\rho c_v}{2\kappa}}, \tag{26}$$

we can easily extract the real and imaginary parts, giving the vibration frequency of the plate together with the corresponding attenuation coefficient [5],

$$\mathrm{Re}(\omega_{nm})=\omega_0\left[1+\frac{\Delta_D}{2}\left(1-\frac{6}{\xi^3}\frac{\sinh\xi-\sin\xi}{\cosh\xi+\cos\xi}\right)\right], \tag{27}$$

$$\mathrm{Im}(\omega_{nm})=\omega_0\frac{\Delta_D}{2}\left(\frac{6}{\xi^3}\frac{\sinh\xi+\sin\xi}{\cosh\xi+\cos\xi}-\frac{6}{\xi^2}\right). \tag{28}$$

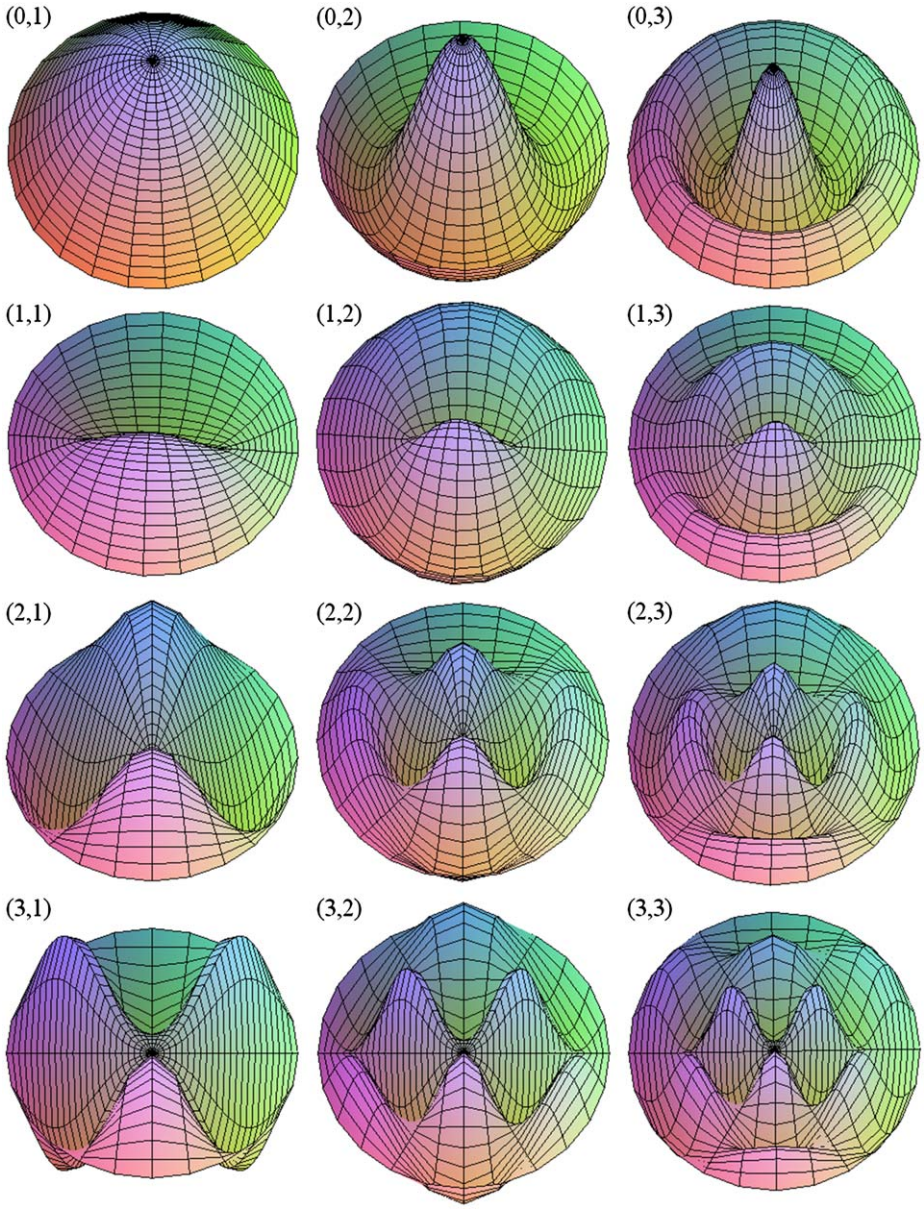

Fig. 1. The first few (n,m) mode shapes of a simply supported circular plate.

Thus we arrive at an expression for thermoelastic damping in a circular plate, which is given by

$$Q^{-1} = 2\left|\frac{\mathrm{Im}(\omega_{nm})}{\mathrm{Re}(\omega_{nm})}\right| = \Delta_D\left(\frac{6}{\xi^2} - \frac{6}{\xi^3}\,\frac{\sinh\xi + \sin\xi}{\cosh\xi + \cos\xi}\right). \tag{29}$$

It can be seen that Eq. (29) has the similar form to the expression of thermoelastic damping in the flexural-mode vibration of a beam resonator, which was obtained by Lifshitz and Roukes [5]. And this is decided by the governing equations.

4. Results and discussions

In this section, the dependency of Q^{-1} on the plate dimensions, boundary conditions, vibration modes and environmental temperatures for silicon MEMS devices are discussed. We use experimentally reported values of the mechanical and thermal parameters of silicon for several representative temperatures: 40, 80, 120, 160, 200, 293 and 400 K,

Table 2
Mechanical and thermal properties of silicon under different temperatures.

T_0 (K)	E (GPa)	ρ (kg m^{-3})	ν	κ (W m^{-1} K^{-1})	c_v (J kg^{-1} K^{-1})	α_T (10^{-6} K^{-1})	χ (10^{-4} m^2 s^{-1})
40	169.3	2330	0.22	3660	44.1	−0.164	356.2
80	169.2	2330	0.22	1360	188	−0.472	31.05
120	169.0	2330	0.22	876	328	−0.057	11.46
160	168.5	2330	0.22	375	456	0.689	3.529
200	166.9	2330	0.22	266	557	1.406	2.050
293	165.9	2330	0.22	156	713	2.59	0.939
400	163.1	2327	0.22	105	785	3.253	0.575

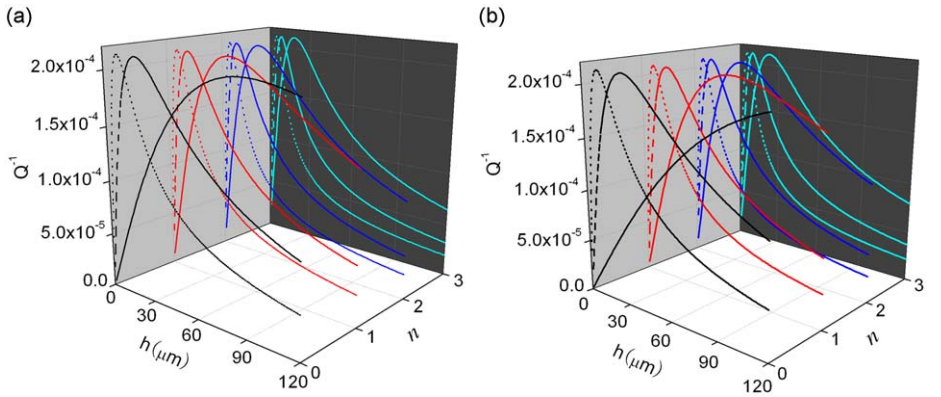

Fig. 2. Thermoelastic damping (n=0, 1, 2, 3 and m=1, 2, 3) of a circular plate against thickness for (a) a clamped plate and (b) a simply supported plate. The aspect ratio of the plate is fixed as a/h=50 and the environmental temperature is T_0=293 K.

Table 3
Critical thickness $h_{nm}{}^c$ (n=0, 1, 2, 3 and m=1, 2, 3) of the clamped and simply supported plates. The aspect ratio is fixed as a/h=50. The unit of $h_{nm}{}^c$ is μm.

n	Clamped			Simply supported		
	h_{n1}^c	h_{n2}^c	h_{n3}^c	h_{n1}^c	h_{n2}^c	h_{n3}^c
0	90.24	23.4	10.44	159.4	30.54	12.43
1	43.77	15.30	7.749	63.38	18.91	8.990
2	26.68	11.00	6.049	35.28	13.13	6.891
3	18.23	8.381	4.889	22.86	9.766	5.493

which are shown in Table 2 [27]. Noting that, in the range of the temperature considered, temperature dependency of thermal properties of silicon, i.e., κ, c_v and α_T are obvious.

First we consider the case of a circular plate with fixed aspect ratio of a/h=50 under the temperature of T_0=293 K. When h is varied, a changes accordingly with h. Fig. 2(a) and (b) shows the thermoelastic damping (n=0, 1, 2, 3 and m=1, 2, 3) of the circular plate against thickness h. Fig. 2(a) presents the values for a clamped plate and Fig. 2(b) for a simply supported plate. The solid, dash and dot lines represent the cases of m=1, 2 and 3, respectively.

It is shown that as the thickness increases, the thermoelastic damping increases first and then decreases, and there is a critical thickness, denoted as $h_{nm}{}^c$, at which the maximum value of thermoelastic damping, denoted as $Q_{\max}^{-1}$, occurs. Table 3 lists the values of $h_{nm}{}^c$ (n=0, 1, 2, 3 and m=1, 2, 3) for the clamped and simply supported circular plates with fixed aspect ratio of a/h=50 under the temperature of T_0=293 K. The maximum value of Q^{-1} are almost the same for both the clamped plate and the simply supported plate. However, in the case of the same vibration mode, the critical thickness for the clamped plate is smaller than that for the simply supported plate. It is shown in Table 3 that $h_{nm}{}^c$ takes the maximum value in the case of n=0 and m=1. When n takes the same value, $h_{nm}{}^c$ takes a smaller value with larger m. Similarly, $h_{nm}{}^c$ decreases with increases of n in the case of the same value of m. That is to say, when the plate vibrates in higher-level mode, $Q_{\max}^{-1}$ occurs in smaller plate.

Fig. 3 plots variation of the thermoelastic damping with ν for a clamped plate with a=500 μm, h=10 μm and T_0=293 K. It is shown that Q^{-1} increases with the increase of ν. However, the variation of Q^{-1} against m changes with n. For example, in

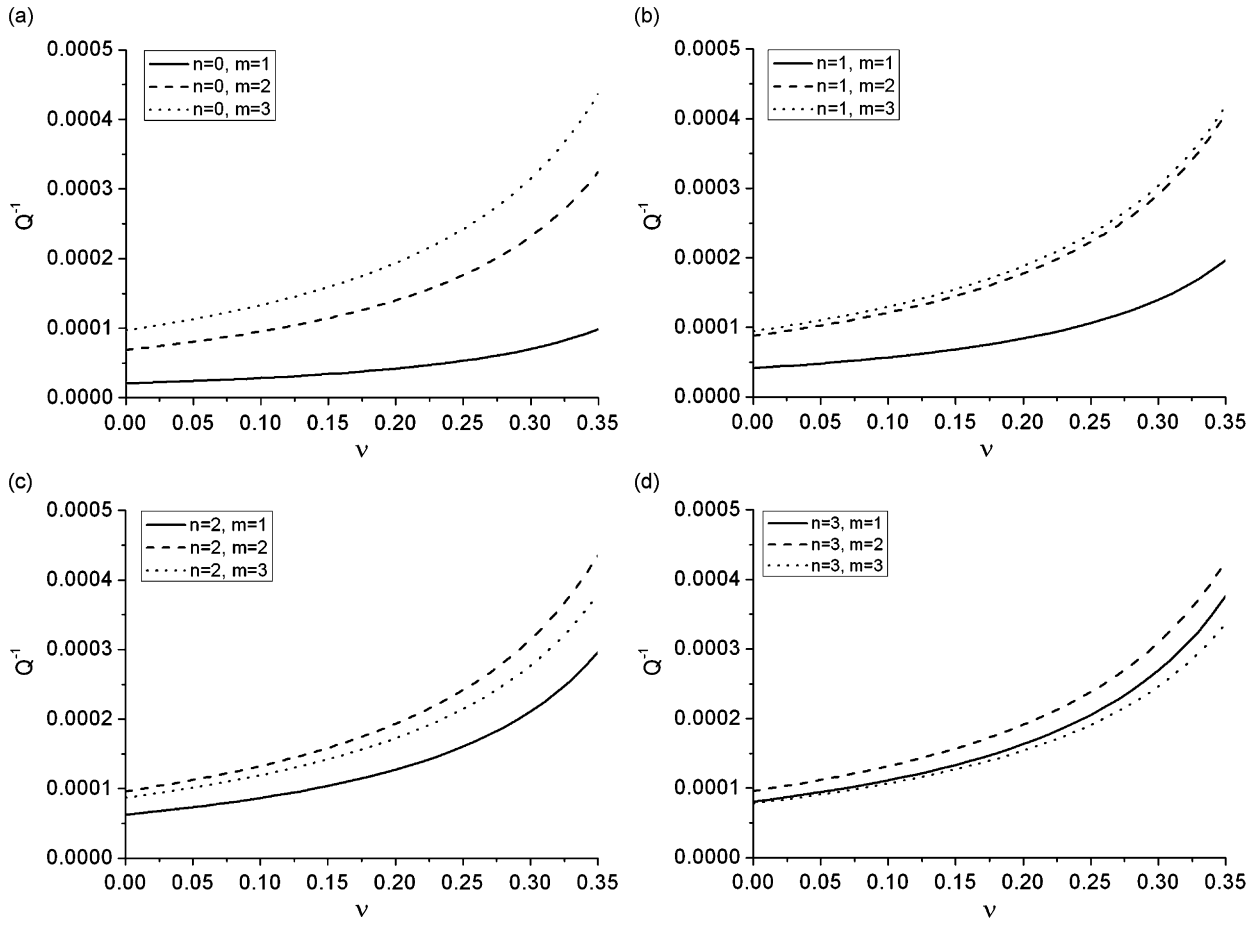

Fig. 3. Variation of the thermoelastic damping with Poisson's ratio ν for a clamped plate with a=500 μm, h=10 μm and T_0=293 K.

the case of n=0, Q^{-1} increases with m; However, in the case of n=3, Q^{-1} of m=2 takes the largest values among the three lines. In the following, we take the value of ν as 0.22.

When n=0, the vibration is axisymmetrical, and it has been discussed in the previous paper [25]. So in the following, we will mainly discuss the case of nonaxisymmetric vibration. In Fig. 4(a)–(c), we plot the dependence of thermoelastic damping on geometries and boundary conditions in three different ways: (a) Q^{-1} against thickness h for fixed aspect ratio of a/h, (b) Q^{-1} against thickness h for fixed radius a, and (c) Q^{-1} against radius a for fixed thickness h. The circular plate is clamped and simply supported, respectively. The outcome is shown for the case of a plate vibrating in the modes of (1,1), (1,2) and (2,1), respectively.

In Fig. 4, it is shown that as the plate size increases, the thermoelastic damping Q^{-1} first increases and then decreases. And there exits a critical size at which Q^{-1} takes the maximum value. In the case of fixed aspect ratio of a/h and fixed radius a, the critical size is the critical thickness, i.e., $h_{nm}{}^c$. It is shown that under the same vibration mode, $h_{nm}{}^c$ of simply supported plate is larger than that of clamped plate. When the plate thickness is larger than the critical thickness, under the same plate thickness and vibration mode, Q^{-1} of simply supported plate is larger than that of clamped plate. On the other hand, under the same boundary conditions, the value of $h_{nm}{}^c$ increases in the sequence of (1, 2), (2, 1) and (1,1) according to (n,m). For a plate with thickness larger than the critical thickness, under the same boundary conditions, the value of Q^{-1} also increases according to the sequence of (n,m) of (1, 2), (2, 1) and (1,1). We can see that the dependencies of $h_{nm}{}^c$ on the boundary conditions and vibration modes show the same tendency as $Q^{-1}$of a plate with thickness larger than the critical thickness. In the case of fixed thickness h, the critical size is the critical radius, i.e., $a_{nm}{}^c$, and the dependencies of $h_{nm}{}^c$ and Q^{-1} on a show an opposite tendency to the above cases.

The dependencies of $h_{nm}{}^c$ on the boundary conditions and vibration modes can be analyzed through the expression of characteristic thickness. It can be seen from Eq. (24) that the frequency without considering the thermoelastic coupling, i.e., ω_0 increases with q_{nm}, which depends on the boundary conditions and the vibration mode. In general terms, this might cause a larger or a smaller Q^{-1}. From Eq. (29), we can see that Q^{-1} takes the maximum value of $Q^{-1}_{\max}$=0.494Δ_D at ξ=2.225. Thus, according to Eqs. (24) and (26), we can obtain the following expression of $h_{nm}{}^c$ for the circular plate with fixed

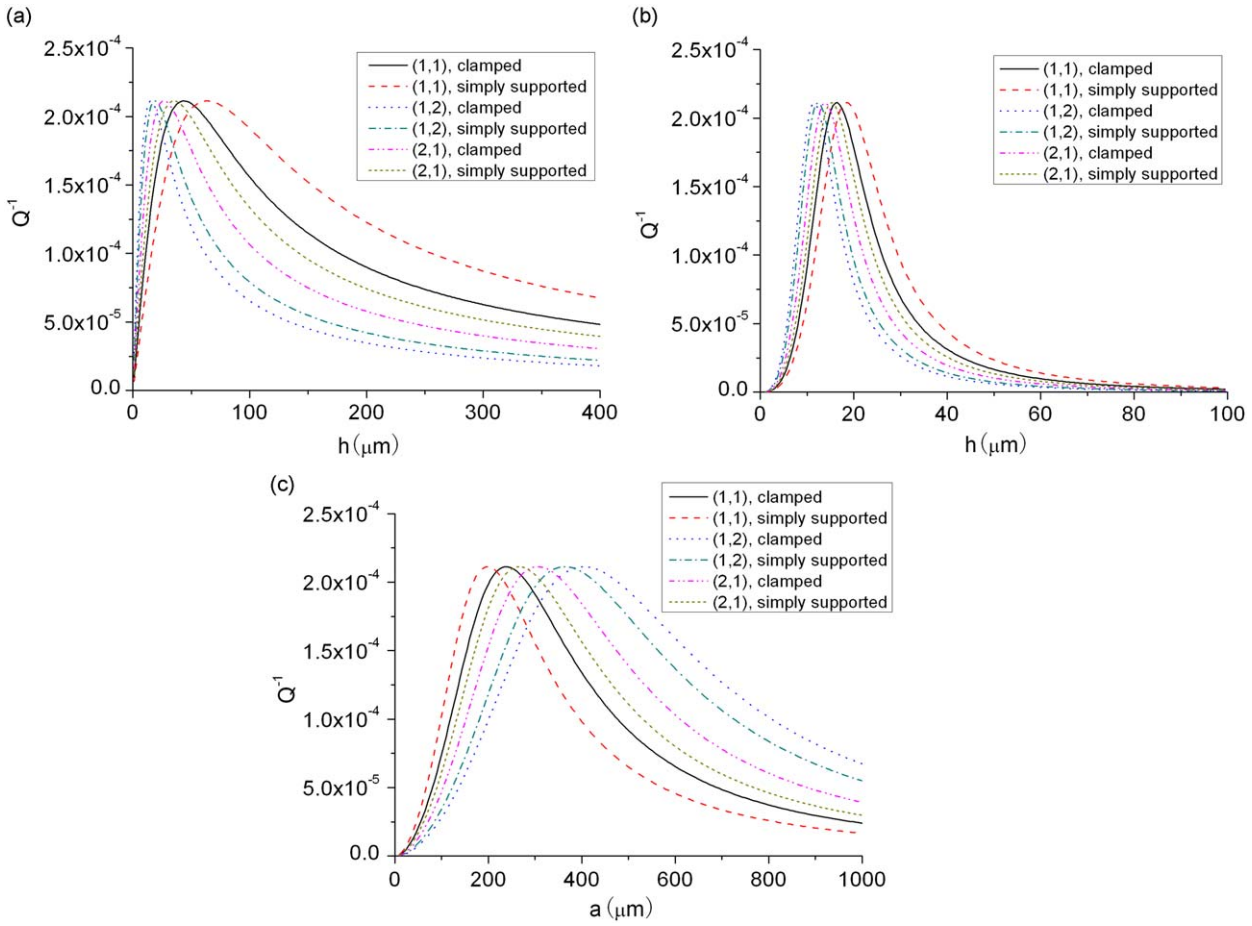

Fig. 4. Thermoelastic damping of the vibration modes of (1, 1), (1, 2) and (2, 1) in a circular plate plotted for different geometries under different boundary conditions: (a) fixed aspect ratio a/h=50, change h; (b) fixed radius a=500 μm, change h; (c) fixed thickness h=10 μm, change a.

aspect ratio of a/h=50:

$$h_{nm}^{c} = \frac{49,500\chi}{q_{nm}}\sqrt{\frac{3\rho(1-\nu^2)}{E}}, \tag{30}$$

where $\chi=\kappa/\rho c_v$ is the thermal diffusion coefficient.

It is shown in Eq. (30) that ${h_{nm}}^c$ decreases with the increase of q_{nm}. And Table 1 shows that q_{nm} gets larger for higher values of n and m.

Next, we consider thermoelastic damping in a clamped plate with fixed aspect ratio of a/h=50 under different temperatures. It is known from Fig. 4 that the tendency of Q^{-1} for simply supported plate is similar to that for clamped plate, so Fig. 5 only shows the case of clamped plate for the purpose of brevity. The outcomes are shown in Fig. 5(a)–(c) for a plate vibrating in the modes of (1,1), (1,2) and (2,1), respectively. The thickness changes in the range of 0.1–500 μm.

First of all, it is shown in Fig. 5 that the thermoelastic damping Q^{-1} under the environmental temperature of T_0=120 K is the smallest. In Gysin's research [28], he tested the internal friction Q^{-1} of the first eigenmode of micro-fabricated silicon cantilevers in the temperature range of 15–300 K and found that the thermoelastic damping depends on temperature clearly and that thermoelastic damping is the smallest under the temperature of 20 and 125 K. Now our calculation demonstrates that this phenomenon is also valid for higher-modes vibration of circular plates.

It can be seen from Fig. 5 that ${h_{nm}}^c$ decreases with increase of temperature. This can also be analyzed through the expression of characteristic thickness. From Eq. (30), we can see that ${h_{nm}}^c$ increases with the increase of χ. The values of χ under different temperatures are listed in Table 2. It is shown that as the temperature increases, χ decreases. As a result, ${h_{nm}}^c$ decreases.

When the environmental temperature, T_0, falls in the range of 120–400 K, the variation of Q^{-1} against h shows the same tendency with that under T_0=293 K, and the value of Q^{-1} increases as T_0 increases. However, Q^{-1} shows different tendency under

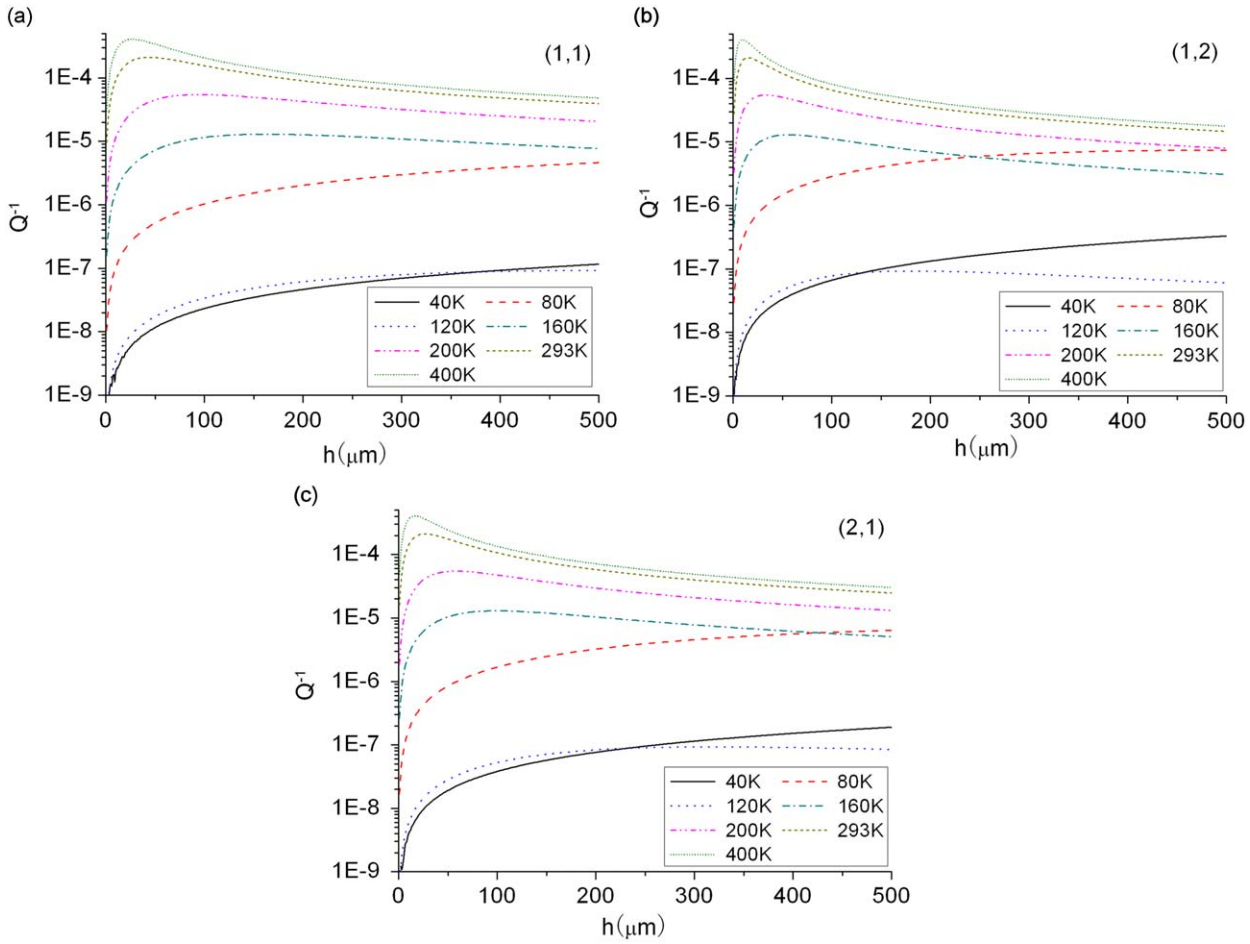

Fig. 5. Variation of the thermoelastic damping with thickness h under different environmental temperature for modes of (a): (1, 1), (b) (1, 2) and (c) (2, 1). The aspect ratio is fixed as a/h=50.

40 and 80 K. It is shown that Q^{-1} continues increasing under T_0=40 K as h increases in the range of 0.1–500 μm. Under T_0=80 K, Q^{-1} first increases quickly and then drops down slowly. According to Eq. (30), the critical thicknesses under 40 and 80 K are 16,438 and 1433 μm, respectively. That is to say, $h_{nm}{}^c$ exceeds the temperature range in discussion under T_0=40 K. As a result, $h_{nm}{}^c$ continues increasing, as is shown in Fig. 5.

5. Conclusions

This paper solved the coupling equations for thermoelastic coupling problem in axisymmetric out-of-plane vibration of circular plate and obtained the analytical expression for thermoelastic damping.

The thermoelastic damping under the environmental-temperature range of 40–400 K is investigated, and it is shown that Q^{-1} depends on temperature clearly. The thermoelastic damping takes the minimum value under 120 K and it increases with temperature under the range of 120–400 K.

In addition, the thermoelastic damping also changes with the plate dimensions and boundary conditions. There is a critical dimension at which the maximum of thermoelastic damping occurs. For a plate with the fixed aspect ratio, the critical dimension decreases as the temperature increases.

The results presented in this paper are based on a quasi-1-D analysis. In the case of beams, a recent 2-D analysis has shown that the 1-D model can lead to errors of up to 80% in the estimation of thermoelastic damping [20]. Therefore, future work need to consider 2-D analysis of thermoelastic damping in circular plates to assess the accuracy of the results presented in this paper. However, the present quasi-1-D analysis was simple and convenient, and we can still get some useful information from the present results and to guide the design of the microscale resonators.

Acknowledgement

This work was supported by Grant-in-Aid for JSPS Fellows 19 07097 and Fanzhou Youth Science Foundation (no. 20090505).

References

[1] J.R. Barnes, R.J. Stephenson, M.E. Welland, C.H. Gerber, J.K. Gimzewski, Photothermal spectroscopy with femtojoule sensitivity using a micromechanical device, *Nature* 372 (1994) 79–81.
[2] R.E. Mihailovich, J.M. Parpia, Low temperature mechanical properties of boron-doped silicon, *Physical Review Letters* 68 (1992) 3052–3055.
[3] D. Zook, W. Burns, R. Herb, H. Guckel, W. Kang, Y. Ahn, Optically excited self-resonant microbeams, *Sensors and Actuators A* 52 (1996) 92–98.
[4] A.N. Cleland, M.L. Roukes, Fabrication of high frequency nanometer scale mechanical resonators from bulk Si crystals, *Applied Physics Letters* 69 (1996) 2653–2655.
[5] R. Lifshitz, M.L. Roukes, Thermoelastic damping in micro- and nanomechanical systems, *Physical Review B* 61 (2000) 5600–5609.
[6] R.E. Mihailovich, N.C. MacDonald, Dissipation measurements of vacuum-operated single-crystal silicon microresonators, *Sensors and Actuators A* 50 (1995) 199–207.
[7] C.L. Zhang, G.S. Xu, Q. Jiang, Analysis of the air-damping effect on a micromachined beam resonator, *Mathematics and Mechanics of Solids* 8 (2003) 315–325.
[8] D.A. Harrington, P. Mohanty, M.L. Roukes, Energy dissipation in suspended micromechanical resonators at low temperatures, *Physica B* 284–288 (2000) 2145–2146.
[9] Y.X. Sun, D.N. Fang, A.K. Soh, Thermoelastic damping in micro-beam resonators, *International Journal of Solids and Structures* 43 (2006) 3213–3229.
[10] C. Zener, Internal friction in solids I. Theory of internal friction in reeds, *Physical Review* 52 (1937) 230–235.
[11] C. Zener, Internal friction in solids II. General theory of thermoelastic internal friction, *Physical Review* 53 (1938) 90–99.
[12] B.S. Berry, Precise investigation of the theory of damping by transverse thermal currents, *Journal of Applied Physics* 26 (1955) 1221–1224.
[13] R.V. Roszhardt, The effect of thermoelastic internal friction on the *Q* of micromachined silicon resonators, *IEEE Solid State Sensor and Actuator Workshop*, Hilton Head Island, SC, USA, June 1990, pp. 13–16.
[14] K.Y. Yasumura, T.D. Stowe, T.W. Kenny, D. Rugar, Thermoelastic energy dissipation in silicon nitride microcantilever structures, *Bulletin of the American Physical Society* 44 (1999) 540.
[15] B.H. Houston, D.M. Photiadis, J.F. Vignola, M.H. Marcus, X. Liu, D. Czaplewski, L. Sekaric, J. Butler, P. Pehrsson, J.A. Bucaro, Loss due to transverse thermoelastic currents in microscale resonators, *Materials Science and Engineering A* 370 (2004) 407–411.
[16] V.T. Srikar, S.D. Senturia, Thermoelastic damping in fine-grained polysilicon flexural beam resonators, *IEEE Journal of Microelectromechanical Systems* 11 (2002) 499–504.
[17] S.J. Wong, C.H.J. Fox, S. McWilliam, Thermoelastic damping of the in-plane vibration of thin silicon rings, *Journal of Sound and Vibration* 293 (2006) 266–285.
[18] Sudipto K. De, N.R. Aluru, Theory of thermoelastic damping in electrostatically actuated microstructures, *Physical Review B* 74 (2006) 144305.
[19] Ali H. Nayfeh, Mohammad I. Younis, Modeling and simulations of thermoelastic damping in microplates, *Journal of Micromechanics and Microengineering* 14 (2004) 1711–1717.
[20] S. Prabhakar, S. Vengallatore, Theory of thermoelastic damping in micromechanical resonators with two-dimensional heat conduction, *Journal of Microelectromechanical Systems* 17 (2008) 494–502.
[21] G. Bao, W. Jiang, A heat transfer analysis for quartz microresonator IR sensors, *International Journal of Solids and Structures* 35 (1998) 3635–3653.
[22] J.R. Vig, R.L. Filler, Y. Kim, Uncooled IR imaging array based on quartz resonators, *IEEE Journal of Microelectromechanical Systems* 5 (1996) 131–137.
[23] H. Ziegler, J. Tiesmeyer, Digital sensor for IR radiation, *Sensors and Actuators A* 4 (1983) 363–367.
[24] M.R. Hamrour, S. Galliou, Analysis of the infrared sensitivity of a quartz resonator application as a thermal sensor, *Proceedings of the Ultrasonic Symposium*, Vol. 36, Cannes, France, 1994, pp. 513–516.
[25] Y.X. Sun, H. Tohmyoh, Thermoelastic damping of the axisymmetric vibration of circular plate resonators, *Journal of Sound and Vibration* 319 (2009) 392–405.
[26] H.N. Arafat, A.H. Nayfeh, W. Faris, Natural frequencies of heated annular and circular plates, *International Journal of Solids and Structures* 41 (2004) 3031–3051.
[27] The Institution of Electrical Engineers, *Properties of Silicon*, INSPEC, London, New York, 1988.
[28] U. Gysin, S. Rast, E. Meyer, D.W. Lee, P. Vettiger, C. Gerber, Temperature dependence of the force sensitivity of silicon cantilevers, *Physical Review B* 69 (2004) 045403.